ヒトへの外挿を目指したナノマテリアルの健康影響評価手法の開発

平成25年度　厚生労働科学研究費補助金

化学物質リスク研究事業

H24－化学－一般－004

平成25年度　総括・分担研究報告書

研究代表　武田　健

平成26年5月

目　次

厚生労働科学研究費補助金（化学物質リスク研究事業）
（H24－化学－一般－004）研究成果(見込み)の概要

「ヒトへの外挿を目指したナノマテリアルの健康影響評価手法の開発」に関する研究
研究代表者:武田　健(東京理科大学総合研究機構教授)

研究要旨：　本プロジェクトではげっ歯類ならびに霊長類モデルを用いて、ナノマテリアルの妊娠期曝露による次世代の免疫系、中枢神経系、雄性生殖系に生じる影響の詳細を検証している。これにより、ナノマテリアル（低用量曝露を含む）の次世代影響に焦点を当てたリスク評価法を確立することを目指している。具体的には、①低用量のナノマテリアルによる次世代雄性生殖系への影響評価、②ナノマテリアルの妊娠期曝露による次世代免疫系・中枢神経系への影響評価指標探索、③ナノマテリアルによる霊長類リンパ節・中枢神経系への影響評価指標探索を目的として研究を進めている。最終年度に二年度目までの結果を総括しながら、In vivo だけでなく ex vivo のナノマテリアル健康影響評価系の構築を目指す。

研究分担者
グループ1
梅澤雅和　東京理科大学　講師
新海雄介　東京理科大学　研究員
立花　研　日本薬科大学　講師
菅又昌雄　栃木臨床病理研究所　所長
井原智美　栃木臨床病理研究所　部長
グループ2
中村 伸　NPO ﾌﾟﾗｲﾒｲﾄｱｺﾞﾗ　所長
光永総子　NPO ﾌﾟﾗｲﾒｲﾄｱｺﾞﾗ　部長

A. 研究目的

本研究課題は、ナノマテリアルの健康影響について特に、1)低用量曝露による次世代雄性生殖系への影響、2)次世代の免疫系・中枢神経系への影響、3)霊長類免疫系・中枢神経系に対する影響を明らかにしようとするものである。1)では妊娠期におけるナノマテリアルの低用量曝露が次世代に及ぼす影響について、次世代の雄性生殖系機能をマーカーとしたげっ歯類の影響評価系の確立を目指している。2)3)を通して、ナノマテリアルが免疫系に及ぼす影響について、ヒトに外挿できる霊長類及びげっ歯類の評価系を確立することを目指している。

B. 研究方法

<u>げっ歯類(マウス)を用いた研究</u>

妊娠マウス(ICR 系、C57BL/6 系)にナノマテリアルを投与した。材料は、生産量が多く汎用されているもののうち、カーボンブラックおよび酸化チタンを用いた。とくに酸化チタンは、アルミナコーティングにより表面性状の異なるものの影響を比較検討した。酸化チタンナノ粒子は懸濁液を皮下、炭素(カーボンブラック)ナノ粒子は懸濁液を気道(点鼻)に投与した。なお、懸濁媒中でのナノ粒子

の存在状態は透過及び走査型電子顕微鏡、ならびに動的光散乱法(DLS)により解析した。その結果、とくに低濃度(低用量投与)のナノ粒子懸濁液については、マテリアルが二次粒子径も100nm未満というスケールに収まっていることを確認した。投与したナノ粒子の動態については、とくに胎仔への移行を透過型電子顕微鏡ならびに走査型電子顕微鏡ーエネルギー分散型X線スペクトロ測定装置(FE-SEM/EDS)により解析した。

次世代雄性生殖器への影響は、母体に投与したナノ粒子の移行・蓄積ならびに精子・精巣の超微小形態の観察により評価した。次世代免疫系への影響は、フローサイトメトリーを用いたリンパ球組成の解析と遺伝子発現解析(機能的トランスクリプトミクスならびに定量的RT-PCR)により評価した。併せて、産仔の免疫系組織及び血液中 miRNA の網羅的解析を行った。さらに、二酸化チタンナノ粒子の次世代影響標的として有力な脳において、影響発現メカニズムをエピジェネティクスの観点から明らかにするために、脳組織における DNA メチル化プロファイルを網羅的に解析した。

(倫理面への配慮)

げっ歯類動物実験は、東京理科大学倫理委員会での承認を得、文部科学省「研究機関等の動物実験等の実施に関する基本指針」、東京理科大学動物実験指針を遵守して行った。ナノ粒子の安全性が不明であることから、P2 プラスレベルの実験に準じた作業手順を実施した。

霊長類(サル)を用いた研究

アカゲザル新生仔の背部皮内に、ナノ材料としてディーゼル排気ナノ粒子(DEP)、非金属ナノ粒子(カーボンブラック:CB)、酸化金属ナノ粒子(二酸化チタン:TiO_2)、蛍光ナノポリスチレン(PS)のいずれかをそれぞれ投与し、1 ヶ月～3年後に投与部位、リンパ節、主要組織の試料を採取した。試料からRNAを抽出した後、遺伝子の発現変動をマイクロアレイ及び定量的 RT-PCR により解析し、その機能的特徴を明らかにした。

C. 研究成果

H25 年度成果

1)次世代雄性生殖系への影響

妊娠マウス1匹あたり0.5μg(ヒト換算で約 0.5～1mg／人)という低用量(高分散性)で、二酸化チタンの仔への移行と影響が生じることを明らかにした。酸化チタンの次世代個体への移行は、電子顕微鏡だけでなく X 線スペクトルによる元素同定により厳密に検出した。次世代の雄性生殖器に移行・蓄積する二酸化チタンナノ粒子は、いずれも二次粒子径(凝集体としての直径)が200 nm以下であることが明らかになった(Kubo-Irie et al. J Nanopart Res 2014)。

さらに、汎用性が高くヒトへの推定曝露量の高い銀ナノ粒子について、その妊娠期投与(飲水投与)による次世代雄性生殖系への影響の検証を始めている。

2)次世代免疫系・中枢神経系への影響

ナノマテリアルの妊娠期曝露による次世代免疫系への影響を、胸腺及び二次リンパ組織の変化に焦点を当てて進めた。とくに、炭素系ナノマテリアルの妊娠前期の投与(経気道)では、次世代新生児の二次リンパ組織の T 細胞比率を低下させるが、妊娠中～後期の曝露では逆に虹リンパ組織の T 細胞が増加す

ることが明らかになった。妊娠期間中の曝露時期の違いによる、次世代免疫系への影響の差異の詳細を現在検討している。

とくにカーボンブラックナノ粒子の妊娠前期の投与によっては、新生児マウスの脾臓中 CD3 陽性(T)リンパ球の減少とともに、T リンパ球の分化・成熟の場である胸腺における転写因子 GF1 ならびに NFI1 に関わる遺伝子群の発現低下が認められた。これは、ナノ粒子の妊娠期曝露により生じる次世代影響を「短期間で未知の毒性も含めて」評価するための網羅的 RNA 発現プロファイルデータ解析手法を開発したことにより得られた成果である。(**日本薬学会 環境・衛生部会部会賞・金原賞受賞、梅澤雅和、2013年9月**)

また、二酸化チタンによる次世代中枢神経系への影響について、その機序を DNA メチル化プロファイルの変動から明らかにすることを目指している。次世代新生児の脳における DNA メチル化レベルは、二酸化チタンナノ粒子の妊娠期投与(経気道)によりゲノム全体にわたって低下する傾向が認められた。それに伴い発現変動した mRNA 群の機能的特徴を検証した結果、G タンパク質共役系などのシグナル伝達系や免疫系に関与するものが抽出され、これらの機能への影響が示唆された。

なお、二酸化チタンナノ粒子の妊娠期曝露は、次世代(産仔)の脳の前頭皮質ならびに線条体におけるドーパミン及びその代謝物を増加させたが(**2013 年ファイザー賞受賞**)、酸化亜鉛の妊娠期曝露はドーパミン代謝物量を増加させた一方で、ドーパミン自体の量は増加させなかった。

3)霊長類を用いた検討(中村 伸)

サル類とげっ歯類との比較発現解析から、リンパ節/免疫系ならびに中枢神経系への影響の分子機序を検討した。さらに、霊長類(ヒトを含む)での ex vivo あるいは semi-in vitro でのナノマテリアル影響評価系についても予備検討した。

その結果、サル・ラット双方において、ナノマテリアルが Dendritic cell /Macrophage の T-cell 活性化制御因子である DC-Hil/GPNMB を顕著に発現亢進することを新たに見出した。ナノマテリアルが T-Cell レベルの免疫応答にも影響することが明らかになった。

D. 考察

「次世代雄性生殖系への影響解析」では、妊娠期マウスに投与した極めて低用量の酸化チタンを次世代の精巣組織内に検出できることを示した。ここで用いた X 線解析の手法(EDS)を用いて、次世代へのナノ粒子の蓄積が他の臓器でも検出できるのかを確認する必要がある。この蓄積が組織特異的であれば、ナノマテリアルの次世代影響自体が組織特異的である(少なくとも程度に偏りがある)可能性を示唆することになる。一方で、他の臓器にも次世代個体中での蓄積が認められれば、ナノマテリアルの次世代影響は全身性に生じる可能性が示唆されることになる。この点は今後の研究により検証する必要がある。なお、本研究グループによる予備的検討の結果では二酸化チタンナノ粒子の妊娠期投与の後、その粒子は次世代の精巣および脳だけでなく、肝臓ならびに腎臓で検出されるのではないかというデータを得ている。また、ナノ粒子が母体に及ぼす影響が二次的に次世代影響を及ぼすことも指摘されており、次世代を対象にしたナ

ノマテリアルのリスク評価については、この点も検討課題である。

また、ナノ粒子による次世代影響は仔への移行・蓄積だけでなく、それに伴いどのような影響が生じるのかという機能的な解析が必須である。現在のところ、ナノ粒子の次世代影響としての機能的変化は不明な点が多いが、「次世代免疫系・中枢神経系への影響解析」で示した“機能的トランスクリプトミクス解析”（遺伝子アノテーションを活用）を駆使してこれが明らかになることにより、ナノマテリアルの次世代影響のリスク評価に利用できるエンドポイントの創出に迫ることができる期待される。すでに、げっ歯類を用いた研究で確率した本手法の、霊長類を用いた研究への応用を進めている。

本研究の大きな特色は、ヒトに外挿可能なリスク評価系を確立するために、霊長類モデルを活用している点である。本プロジェクトでは、げっ歯類モデルで得られる多くのデータ・知見の霊長類モデルでの検証を進め、ヒトへの外挿可能性を考察していくことが必要であると考えている。本研究プロジェクトを通して、網羅的RNA 発現プロファイルの機能解析技術を確立しつつある。これにより、本プロジェクトでは新たなナノマテリアル影響評価指標及びナノマテリアルの標的細胞種の探索を進めるとともに、サルモデルのデータを踏まえたヒトへの外挿性の高いナノマテリアル生体影響評価手法（*in vivo*、*ex vivo*）を構築することを目指す。

E. 結論

本研究課題では、ナノマテリアルの健康影響について、1）次世代雄性生殖系への影響解析、2）次世代免疫系への影響解析を通して次世代影響の短期間（新生児マウス）での評価、ならびに、3）霊長類免疫系に及ぼす影響解析を通して、ヒトへの外挿が可能な低用量ナノマテリアルによる影響の鋭敏かつ定量的な評価を実現しつつある。さらに、トランスクリプトミクス及びその機能的解析により、未知の毒性も含めて低コストで検出できる評価系を確立できると考えている。
本プロジェクトの成果として、ヒトに外挿可能なナノマテリアルの健康影響評価系（胎児や新生児という高感受性集団への影響評価を含む）を確立することにより、国民の健康・安全を守ることとナノテクノロジー産業の健全な発展との両立に貢献できると期待している。

F. 研究発表

1．論文発表

1. Onoda A, Umezawa M, Takeda K, Ihara T, Sugamata M. (2014) Effects of maternal exposure to ultrafine carbon black on brain perivascular macrophages and surrounding astrocytes in offspring mice. PLoS One, 9(4): e94336（査読有）

2. Kubo-Irie, M., Uchida, H., Mastuzawa, S., Yoshida, Y., Shinkai, Y., Suzuki, K., Yokota, S., Oshio,S., Takeda, K. (2014) Dose-dependent biodistribution of prenatal exposure to rutile-type titanium dioxide nanoparticles on mouse testis. J. Nanoparticle Res. 16 : 2284

3. Suzuki.K, Adigüzel.D, Shinotsuka.T, Ishibashi.R, Eguchi.I, Oshima.H, Taniguchi.R, Thalhammer. S, Takeda. K,. (2014)Tunable plasma lipoprotein uptake/transport across the blood-brain barrier. Colloids and Surfaces A.442:157-163

4. Umezawa M, Sekita K, Suzuki K, Kubo-Irie M, Niki R, Ihara T, Sugamata M, takeda K.(2013) Effect of aerosol particles generated by ultrasonic humidifiers on the lung in mouse. Part Fibre Toxicol 10: 64

5. Yokota.S, Hori.H, Umezawa.M, Kubota.N, Niki.R, Yanagita.S, Takeda.K,. (2013)

Gene expression changes in the olfactory bulb of mice induced by exposure to diesel.exhaust are dependent on animal rearing environment. PLOS ONE.8(8):e70145.

6. Okada .Y, Tachibana. K, Yanagita. S, Takeda. K. (2013) Prenatal exposure to zinc oxide particles alters monoaminergic neurotransmitter levels in the brain of mouse offspring. Journal of Toxicological Sciences, 38(3):363-370.

7. 梅澤雅和 (2013) ナノ粒子の健康リスク (2) 私たちはいかにリスクを回避できるのか 市民研通信（市民科学研究室・上田昌文ら編)、第17号＝通巻145号

8. 梅澤雅和 (2013) 薬学・情報学・社会学をつないで切り拓く次世代健康科学、東京理科大学 科学フォーラム 2013(6)14-17

9. 立花 研 (2013) 小さなRNAから環境化学物質と次世代の健康を考える、東京理科大学 科学フェーラム 2013(6)18-21

10. 梅澤雅和、武田 健 (2013) PM2.5の健康影響について 私たちが注意したいこと（科学2013年4月号）岩波書店、Vol.83.NO.4. 424-427.

11. Yokota S, Moriya N, Iwata M, Umezawa M, Oshio S, Takeda K. (2013) Exposure to diesel exhaust during fetal period affects behavior and neurotransmitters in male offspring mice. Journal of Toxicological Sciences, 38(1): 13-23.

2．学会発表

1. 小野田淳人、梅澤雅和、武田健、井原智美、菅又昌雄「炭素ナノ粒子の胎仔期曝露が脳血管周囲マクロファージ及びアストロサイトに及ぼす影響」、『日本薬学会第 134 年会』、熊本、2014 年 3 月 27 日～30 日

2. 立花 研、高柳皓平、秋本純芽、上田剛司、新海雄介、梅澤雅和、武田 健「ディーゼル排ガス胎仔期曝露により脳に生じる DNA メチル化異常の解析」、『日本薬学会第 134 年会』、熊本、2014 年 3 月 27 日～30 日

3. 梅澤雅和、岡本沙紀、小野田淳人、清水隆平、小川修平、渡辺志帆、安部良、武田 健「カーボンブラックナノ粒子が次世代免疫系に及ぼす影響の投与時期による違い」、『日本薬学会第 134 年会』、熊本、2014 年 3 月 27 日～30 日

4. Umezawa M, Shimizu M, Tainaka H, Takeda K. Maternal exposure to titanium dioxide nanoparticle affects gene expression in the brain development 6th International Symposium on Nanotechnology, Occupational and Environmental Health (NanOEH) (Nagoya, Japan), October29-31,2013

5. Okamoto S, Umezawa M, Shimizu R, Onoda A, Uchiyama M, Watanabe S, Ogawa S, Abe R, Takeda K. Effect of treatment of pregnant mice with carbon black nanoparticle on the neonatal immune system 6th International Symposium on Nanotechnology, Occupational and Environmental Health (NanOEH) (Nagoya, Japan), October29-31,2013

6. Onoda A, Umezawa M, Takeda K, Ihara T, Sugamata M. Maternal exposure to carbon black nanoparticle affects perivascular cells in the brain of offspring 6th International Symposium on Nanotechnology, Occupational and

Environmental Health (NanOEH) (Nagoya, Japan), October29-31,2013

7. Tachibana K, Kojima T, Kuroiwa N, Yuasa T, Umezawa M, Takeda K. Effect of prenatal exposure to titanium dioxide nanoparticle on miRNA expression in mouse embryo 6th International Symposium on Nanotechnology, Occupational and Environmental Health (NanOEH), Session "Health effects and toxicity - in vivo" (Nagoya, Japan), October29-31,2013

8. 梅澤雅和、ナノ材料の次世代健康影響－疾病予防を目指した研究と取り組み、知の市場、ナノ材料総合管理、東京、2013 年 10 月 24 日

9. Sugamata M, Ihara T, Sugamata M, Ying Ji Li, Yamamoto M, Takeda K, Nrf2 Lowers Risk for Neurodegenerative Diseases Caused by Oxidative Stresses Induced by Disel Exhaust. American Neurological Association. New Orleans, October13-15,2013

10. 梅澤雅和、鈴木智晴、押尾　茂、武田健、ディーゼル排ガスの妊娠期曝露が次世代マウスの自発運動量及びドーパミン系神経伝達に及ぼす影響、第 54 回大気環境学会年会、新潟、2013 年 9 月 18～20 日

11. 梅澤雅和、岡本沙紀、清水隆平、武田健、カーボンブラックナノ粒子の妊娠期曝露が次世代リンパ組織に及ぼす影響、フォーラム 2013 衛生薬学・環境トキシコロジー、福岡、2013 年 9 月 13 日～14 日

12. 上田剛司、立花　研、高柳皓平、秋本純芽、新海雄介、武田　健、ディーゼル排ガス胎仔期曝露による DNA メチル化状態の網羅的解析、フォーラム 2013 衛生薬学・環境トキシコロジー、福岡、2013 年 9 月 13 日～14 日

13. 曽我勇介、新海雄介、荒舩　亮、入江美代子、武田　健、妊娠マウスへの銀ナノ粒子経口投与が産仔精子形態に及ぼす影響、フォーラム 2013 衛生薬学・環境トキシコロジー、福岡、2013 年 9 月 13 日～14 日

14. Umezawa M, Shimizu M, Tainaka H, Takeda K. Estimation of brain regions targeted by nanoparticle based on transcriptomics data. FENS Featured Regional Meeting, Prague, Czech Republic（2013 年 9 月 11 日～14 日）

15. Yoshida A, Yoshikawa Y, Umezawa M, Suzuki K, Takeda K. GLI2-activation by apolipoprotein B regulates gliogenesis in the postnatal cerebral cortex. FENS Featured Regional Meeting, Prague, Czech Republic（2013 年 9 月 11 日～14 日）

16. Yoshikawa Y, Yoshida A, Umezawa M, Suzuki K, Takeda K. Methodological development of isolation and culture of protoplasmic astrocytes. FENS Featured Regional Meeting, Prague, Czech Republic（2013 年 9 月 11 日～14 日）

17. Taniguchi R, Suzuki K, Yoshida A, Yoshikawa Y, Umezawa M, Takeda K. Novel fabrication method of

biocompatible nanoparticles for theranostic applications. 27th Conference of ECIS (European Colloid and Interface Society), Sofia, Bulgaria（2013 年 9 月 1 日～6 日）

18. 湯浅珠恵、立花　研、小島稔郁、武田健、妊娠期の酸化チタンナノ粒子曝露による羊水中マイクロ RNA 発現変動の解析、第 5 回日本 RNAi 研究会、広島、2013 年 8 月 29 日～31 日

19. 小島稔郁、立花　研、黒岩法子、新海雄介、武田　健、妊娠期の酸化チタンナノ粒子曝露による胎盤のマイクロ RNA 発現量の変動の解析、第 5 回日本 RNAi 研究会、広島、2013 年 8 月 29 日～31 日

20. 落合紘子，柳田信也，久保田夏子，高野由莉香，武田　健，ディーゼル排ガス胎仔期曝露が大脳皮質発達過程に影響を及ぼす. Neuro2013(第 36 回日本神経科学大会、第 56 回日本神経化学会大会、第 23 回日本神経回路学会大会、合同大会)、京都、2013 年 6 月 20 日～23 日

21. Umezawa M, Shimizu R, Okamoto S, Takeda K. Effect of prenatal exposure to carbon black nanoparticle on gene expression in the thymus of offspring mouse during neonatal period. 10th International Particle Toxicology Conference (IPTC2013), Düsseldorf, Germany（2013 年 6 月 4 日～7 日）

22. Tachibana K, Kawazoe S, Umezawa M, Takeda K. Effect of prenatal exposure to titanium dioxide nanoparticle on the gene expression in the brain of mouse offspring. 10th International Particle Toxicology Conference (IPTC2013), Düsseldorf, Germany（2013 年 6 月 4 日～7 日）

23. 吉川洋一郎、鈴木健一郎、武田　健、リン脂質被覆ナノ粒子表面に結合する血漿中タンパク質の同定、第 73 回分析化学討論会、函館、2013 年 5 月 18～19 日

３．招待講演

1. 梅澤雅和、ナノ材料の次世代健康影響－疾病予防を目指した研究と取り組み、知の市場、ナノ材料総合管理、東京、2013 年 10 月 24 日

2. 梅澤雅和、ディーゼル排ガス・大気中の微小な粒子と子どもの健康、大気汚染測定運動東京連絡会　第 72 回報告集会、東京、2013 年 10 月 5 日

3. Umezawa M, Takeda K. From toxicology to sociology – effects of nanoparticles on children's health and the next generation 2nd International Postgraduate Conference on Pharmaceutical Sciences (iPoPS 2013), Session "Pharmaceutical Chemistry" (Universiti Teknologi MARA (UiTM), Puncak Alam, Selangor, Malaysia), September 2013.

4. 梅澤雅和、網羅的遺伝子発現データの機能的解析によるカーボンブラックナノ粒子の次世代免疫系への影響評価、フォーラム 2013 衛生薬学・環境トキシコロジー、福岡、2013 年 9 月 13 日～14 日

5. Umezawa M, Takeda K. From toxicology

to sociology -- Effects of nanoparticles on children's health and the next generation. iPoPS 2013 (2nd International Postgraduate Conference on Pharmaceutical Sciences), Puncak Alam Campus, UiTM, Malaysia（2013 年 9 月 4 日～5 日）

H. 知的財産権の出願・登録状況

なし

Effects of Maternal Exposure to Ultrafine Carbon Black on Brain Perivascular Macrophages and Surrounding Astrocytes in Offspring Mice

Atsuto Onoda[1,2]*, Masakazu Umezawa[1,3], Ken Takeda[1,3], Tomomi Ihara[2], Masao Sugamata[2]

1 Department of Hygienic Chemistry, Faculty of Pharmaceutical Sciences, Tokyo University of Science, Noda, Chiba, Japan, **2** Department of Pathology, Tochigi Institute of Clinical Pathology, Nogi, Tochigi, Japan, **3** The Center for Environmental Health Science for the Next Generation, Research Institute for Science and Technology, Tokyo University of Science, Noda, Chiba, Japan

Abstract

Perivascular macrophages (PVMs) constitute a subpopulation of resident macrophages in the central nervous system (CNS). They are located at the blood-brain barrier and can contribute to maintenance of brain functions in both health and disease conditions. PVMs have been shown to respond to particle substances administered during the prenatal period, which may alter their phenotype over a long period. We aimed to investigate the effects of maternal exposure to ultrafine carbon black (UfCB) on PVMs and astrocytes close to the blood vessels in offspring mice. Pregnant mice were exposed to UfCB suspension by intranasal instillation on gestational days 5 and 9. Brains were collected from their offspring at 6 and 12 weeks after birth. PVM and astrocyte phenotypes were examined by Periodic Acid Schiff (PAS) staining, transmission electron microscopy and PAS-glial fibrillary acidic protein (GFAP) double staining. PVM granules were found to be enlarged and the number of PAS-positive PVMs was decreased in UfCB-exposed offspring. These results suggested that in offspring, "normal" PVMs decreased in a wide area of the CNS through maternal UfCB exposure. The increase in astrocytic GFAP expression level was closely related to the enlargement of granules in the attached PVMs in offspring. Honeycomb-like structures in some PVM granules and swelling of astrocytic end-foot were observed under electron microscopy in the UfCB group. The phenotypic changes in PVMs and astrocytes indicate that maternal UfCB exposure may result in changes to brain blood vessels and be associated with increased risk of dysfunction and disorder in the offspring brain.

Citation: Onoda A, Umezawa M, Takeda K, Ihara T, Sugamata M (2014) Effects of Maternal Exposure to Ultrafine Carbon Black on Brain Perivascular Macrophages and Surrounding Astrocytes in Offspring Mice. PLoS ONE 9(4): e94336. doi:10.1371/journal.pone.0094336

Editor: Michelle L. Block, Virginia Commonwealth University, United States of America

Received January 30, 2014; **Accepted** March 12, 2014; **Published** April 10, 2014

Funding: This work was supported in part by a JSPS KAKENHI Grant Number 24790130 (http://www.jsps.go.jp/english/e-grants/; 2012-2013), a MEXT-Supported Program for the Strategic Research Foundation at Private Universities (http://www.mext.go.jp/english/; 2011-2015) and a Grant-in-Aid for the Health and Labour Sciences Research Grant (Research on the Risk of Chemical Substances) from the Ministry of Health, Labour and Welfare (Grant Number 12103301, http://www.mhlw.go.jp/english/; 2012-2014). The funders had no role in study design, data collection and analysis, decision to publish, or preparation of the manuscript.

Competing Interests: The authors have declared that no competing interests exist.

* E-mail: atsutoyukari@gmail.com

Introduction

Resident phagocytes of the central nervous system (CNS) are categorized into four types: microglia, meningeal macrophages, choroid plexus macrophages, and perivascular macrophages (PVMs). These contribute to maintaining homeostasis in the CNS [1,2]. Recently initiated investigations aim to elucidate the characteristics and function of PVMs, also called perivascular cells, perivascular microglia and fluorescent granular perithelial cells [3]. PVMs are localized in the perivascular space (Virchow-Robin space) and are surrounded by the vascular endothelial basement membrane and glia limitans [4,5]. In this space, PVMs adjoin endothelial cells, pericytes [4,5,6], and the end-foot of astrocytes, which are one of the types of cerebral parenchyma glial cells in the surrounding brain microvessels [7,8]. This space plays a particularly important role in the drainage of interstitial fluid containing unnecessary substances and waste including β-amyloid from the central grey matter and cerebral cortex [9,10,11,12]. PVMs encounter various substances, including pathogens and waste from blood flow and brain parenchyma, and play a crucial role in regulating inflammatory responses in the CNS [13]. PVMs are the only cells that display constitutive phagocytic potential in the brain parenchyma [14] that and express immunophenotypical markers of activation such as major histocompatibility class II (MHC II), B7, CD40, and Fc receptor (FcR) [3]. Because of their unique localization, phagocytic function and character PVMs are also essential for maintaining blood brain barrier (BBB) function [15].

Research focused on PVM turnover reported that PVMs are partially and continuously replaced under physiological conditions [3]. Under pathological conditions such as rodent experimental allergic encephalomyelitis, there is a great increase in the number of PVMs accumulated around blood vessels in the brain [8]. Previous studies have also suggested that PVMs respond uniquely to particulate matter. In a rat model, carbon particles injected into the cerebral ventricle were move to perivascular spaces and phagocytosed by PVMs within 1 week. Moreover, the carbon could be detected for more than two years in cells that were laden with particles [14]. These data indicated that it is difficult for PVMs to excrete or dispose of carbon particles and that the presence of these particles may induce some signals or responses in the surrounding cells. This evidence suggested that in PVMs and

their surrounding perivascular spaces, particulate substances may stay and promote biological responses over a long period of time.

The authors aimed to investigate the effects of nano-sized particles because previous studies suggested that they have a greater effect than larger sized particles [16,17,18], especially in the CNS [19] and endothelial cells [20,21]. Because of their small size, nano-sized particles have a larger relative surface area per mass than do bulk-size particles of the same material; this feature often makes nano-sized particles more toxic [22]. Small size of nano-sized particles also enables certain nano-sized particles to cross cell membranes and translocate from the environment into the organism [23]. The lungs and airways are the most important exposure sites for involuntary exposure to nano-sized particles. Respirable nano-sized particles not only elicit local pulmonary effects [24,25,26], but they also can translocate from lung epithelium to extrapulmonary organs [27,28] and developing fetus [29]. It has also been reported that maternal exposure to diesel exhaust particles, which contain nano-sized carbon particles at their core, alters the ultrastructure of PVMs and surrounding tissues in the brain of mouse offspring [30]. This finding suggests that maternal exposure to nano-sized particles may alter the phenotype of PVMs and other cerebral cells in mouse offspring.

The aim of the present study was to investigate the effects of maternal exposure to ultrafine carbon black (UfCB) on the perivascular regions, especially the PVMs and astrocytes close to blood vessels in the brains of the offspring of maternally exposed mice (UfCB-exposed offspring).

Materials and Methods

Ultrafine carbon black

Printex 90, purchased from Degussa Ltd. (Frankfurt, Germany), was used as UfCB. The particle is insoluble in water [31]. The manufacturer reported an average primary particle size of 14 nm and an organic impurity content of less than 1%. The specific surface area was determined to be 295-338 m^2/g [32]. The total carbon content measured was >99 wt%, with 0.82 nitrogen and 0.01 hydrogen wt%. Very low levels of both total polycyclic aromatic hydrocarbon (PAH) (74.2 ng/g) [33,34] and total endotoxin (0.142 EU/mg Printex 90) were detected in the sample.

The UfCB particles were suspended at 5 mg/mL in distilled water, sonicated for 30 min, and then filtered through a 450-nm filter (S-2504; Kurabo Co. Ltd., Osaka, Japan) immediately before administration. The particles in the filtered suspension were characterized by transmission electron microscopy (TEM; JEM 1200EXII, JEOL Ltd., Akishima, Tokyo, Japan) on collodion-coated 200 Cu mesh (Nisshin EM, Cat.No. 6511). The size distribution of secondary UfCB particles in the suspension was determined by dynamic light scattering measurement using a NANO-ZS (Sysmex Co., Kobe, Hyogo, Japan) and the Rayleigh-Debye equation. The UfCB concentration in the suspension was calculated to be 95 μg/mL by peak area of carbon signal (2.77 keV) obtained using a field emission scanning electron microscope (JSM-6500F) with an attached energy-dispersive X-ray analyzer (JSM-6500F).

Animals and treatments

Ten pregnant ICR mice (11 weeks of age) were purchased from SLC Inc. (Hamamatsu, Shizuoka, Japan) and were randomly divided into two groups: UfCB-exposed (n = 5) and control (n = 5). The mice were housed under controlled temperature (23±1°C) and humidity (55%±5%) with a 12-hr dark/light cycle and ad libitum access to food and water. The pregnant mice were put into anesthesia box filled with halothane, and then taken out from the box when they began to sleep. The mice were immediately laid on their back and treated with 1 mL/kg (body weight) of UfCB suspension (95 μg/mL, for UfCB group) or distilled water (for control group) by intranasal instillation into both nostrils. 95 μg/mL was maximum concentration of UfCB suspension without bulk agglomeration or any dispersant. The total dose of UfCB (190 μg/kg body weight) was lower than the doses used in many earlier studies of nano-sized particle effects. The treatment were perfomed on gestational days (GDs) 5 and 9, because the fetus of mice on these days is particularly sensitive to various foreign substances in comparison to any other fetal period [35]. Previous study showed that fetal malformation were observed by maternal exposure to single-wall carbon nanotube on GD 5.5 [36]. Additionally, developmental effect of respiratory exposure to UfCB on kidney was examined by twice intranasal instillation on GDs 5 and 9 in the previous study [37]. The number of pups per dam was adjusted randomly to 11 or 12 on postnatal day 1. After weaning at 3 weeks of age, 4–6 male offspring per dam were randomly selected and used for analysis. Brains were collected from male offspring mice at 6 and 12 weeks after birth (Figure 1). All experiments were performed in accordance with Animal Research: Reporting In Vivo Experiments guidelines for the care and use of laboratory animals [38] and were approved by Tokyo University of Science's Institutional Animal Care and Use Committee. All sampling was performed under sodium pentobarbital (50 mg/kg) anesthesia, and all efforts were made to minimize suffering.

Periodic Acid Schiff (PAS) staining

Brains from 6-week-old (n = 5/group) and 12-week-old (n = 5/group) male offspring mice were fixed in 4% paraformaldehyde and 1% glutaraldehyde, embedded in paraffin and cut into 3-μm sections for analysis with PAS staining to visualize PVM granules. The sections were oxidized in 1% periodic acid solution for 1 min. After rinsing for 3 min in distilled water, the sections were soaked in cold Schiff reagent for 45 min. Next, the sections were soaked in sulphurous acid solution 3 times for 5 min and then rinsed for 3 min in distilled water. Finally, the sections were counterstained in haematoxylin for 1 sec, then washed in flowing tap-water, dehydrated in graded alcohol, cleared in xylene, and coverslips were applied with permount mounting medium (Thermo Fisher Scientific Inc., Weltham, MA,USA).

PAS-positive PVM counting

PAS-positive PVMs were observed in sections using a BX-10 microscope (Olympus, Co., Tokyo, Japan) equipped with a digital camera (BX41; Olympus). Fifty sections (total 150 μm) from the longitudinal fissure of the cerebrum along sagittal plane were prepared from each mouse. One in every 10 sections was chosen (every 30 μm) for analysis by PAS staining. In total, 3 sections per mouse (about 150 μm^2/mouse) were subjected to quantitative analysis (Table S1). Stained sections were photographed by optical microscope at 40X magnification. PAS-positive PVM was confirmed by optical microscope with 400X magnification and plotted on 40X-magnified photographs. The PAS-positive cell number per 1 mm^2 area was calculated for each region.

Transmission electron microscopy (TEM)

Brains which removed from 6 (n = 3/group) and 12 (n = 3/group) week-old male offspring mice were fixed by 4% paraformaldehyde and 1% glutaraldehyde. Fixed tissues were washed with phosphate buffer (pH7.4) and post-fixed with osmium tetroxide. These tissue samples were dehydrated in a graded series of ethanol and propylene oxide, and then embedded in

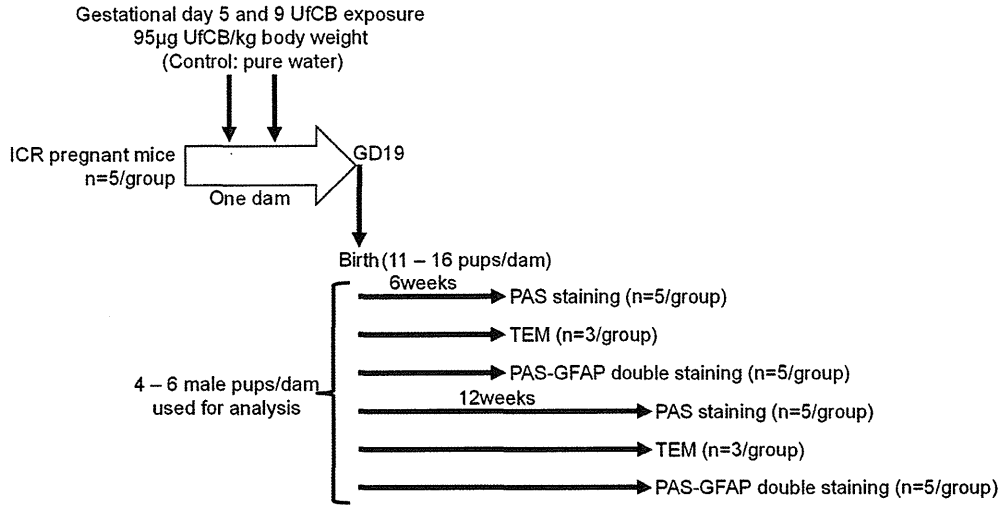

Figure 1. Summarised scheme of animal treatments and sample collection.
doi:10.1371/journal.pone.0094336.g001

epoxy resin (Epon 812, Shell Chemicals Ltd., Houston, TX, USA). Ultrathin sections of each sample were stained with uranyl acetate and lead citrate and examined by transmission electron microscopy (JEOL100-S, JEOL Ltd., Tokyo, Japan) with an accelerating voltage of 80 kV.

Double-staining for GFAP and PAS-positive granules

Brains from 6-week-old (n = 5/group) male offspring mice were used for double-staining for glial fibrillary acidic protein (GFAP) and PAS-positive granules. The brain samples were fixed for 24 hr in 4% paraformaldehyde. Right brains were embedded in paraffin and cut into 6-μm sections for wide-field analysis. Left brains were cryoprotected in phosphate-buffered sucrose solutions (10% sucrose, 4–6 hr; 20% sucrose, 4–6 hr; 30% sucrose, 12–36 hr) with 0.1% sodium azide, embedded in Tissue-Tek OCT compound (Sakura Finetek Japan Co., Ltd., Tokyo, Japan) and then cut into 10-μm frozen sections for observation of detailed morphology.

Visualization of GFAP and PAS-positive granules was performed on paraffin and frozen sections using antibodies and an avidin–biotin-peroxidase method. After blocking endogenous peroxidase and preincubation in 10% normal horse serum, sections were incubated in primary rabbit polyclonal anti-GFAP antibody (Code-No. Z0334, DakoCytomation, Copenhagen, Denmark) diluted 1:1000 in 0.1 M PBS with 0.1% Trion X (PBS-Tx) for 16 hr at 4°C. After rinsing 3 times for 5 min in PBS-Tx, sections were further incubated in secondary biotinylated donkey anti-rabbit IgG (AP182B, Chemicon, Temecula, CA, USA;

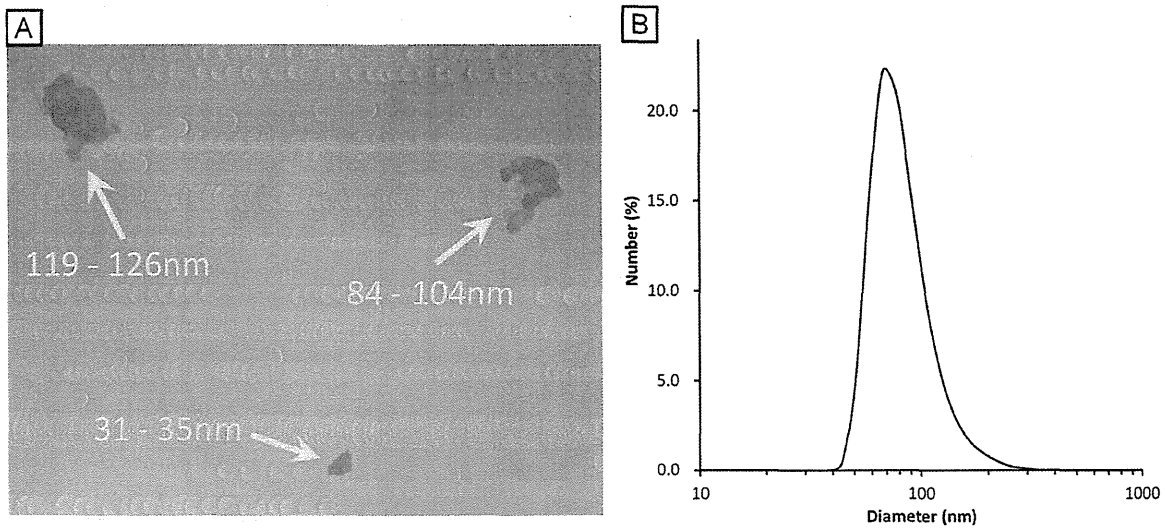

Figure 2. Characterisation of ultrafine carbon black (UfCB). A: Transmission electron microscopy images of UfCB particles in the instillation medium. The yellow numerical value means minor axis - major axis of the secondary UfCB particles. B: Dynamic light scattering data of UfCB in the instillation medium.
doi:10.1371/journal.pone.0094336.g002

Table 1. Number and sex ratio of offspring.

	Number of dams	Number of offspring	Sex ratio (%)*
Control	5	13.8±2.2	46.8±9.8
UfCB	5	13.0±1.2	62.5±21.4

Data are presented as mean ± SD.
*Sex ratio (%) = male/(male + female) ×100
doi:10.1371/journal.pone.0094336.t001

1:1000) for 120 min at room temperature and rinsed 3 times for 5 min in PBS-Tx. The sections were oxidized in 1% periodic acid solution for 3 min, rinsed for 1 min in distilled water, and then soaked in cold Schiff reagent for 60 min. Next, the sections were soaked in sulphurous acid solution 3 times for 3 min and then rinsed for 1 min in distilled water. Finally, the sections were treated with an avidin-biotin-peroxidase complex (Vectastain ABC peroxidase kit, Vector Laboratories Inc., Burlingame, CA, USA; 1:400) for 120 min. The sections were then reacted for peroxidase activity in a solution of 0.02% 3,3′-diaminobenzidene (DAB) in 0.1 M Tris–HCl buffer (pH 7.6) and 0.01% H_2O_2 for 20 min. Immunoreactivity for GFAP was localized to the astrocytic cytoplasm and was visible as light-brown staining. Sections were then washed in 0.1 M PBS, dehydrated in graded alcohol, cleared in xylene, and coverslips were applied with permount mounting medium (Thermo Fisher Scientific).

Statistical analysis

Data are expressed as the mean ± SD. The effects of maternal exposure to UfCB on number and sex ratio of pups at birth were identified by an unpaired t-test, and their body weight at 6 and 12 weeks of age were identified by 2-way ANOVA (Exposure × Age) followed by the Tukey-Kramer post hoc test. For quantitative observation of PAS-positive PVMs, an unpaired t-test was performed. Data analysis was performed using Excel Statistics 2012 for Windows (Social Survey Research Information, Tokyo, Japan). Significance of the difference among means was estimated at $P<0.05$.

Results

UfCB characterisation

The particle suspension (95 μg/mL) was characterised by transmission electron microscopy (TEM) and dynamic light scattering analysis. The TEM analysis of the instillation suspension showed that Printex 90 consisted of open chain-agglomerates of 30–200 nm in diameter (Figure 2A). The filtered Printex 90 suspension, which was employed for intranasal instillation, showed the presence of small agglomerated particles with a peak size of 84.2 nm (Figure 2B). The polydispersity index of 0.143 was low, indicating a narrow size-distribution. This 84.2 nm size corresponds well with the typical small agglomerate sizes of Printex 90 observed under TEM (Figure 2A).

Table 2. Effect of maternal exposure to UfCB on body weight (g) of male offspring at 6 and 12 weeks of age.

	6-week-old male	12-week-old male
Control	33.9±3.0	42.8±3.3
UfCB	33.9±2.1	40.8±5.2

Data are presented as mean ± SD
doi:10.1371/journal.pone.0094336.t002

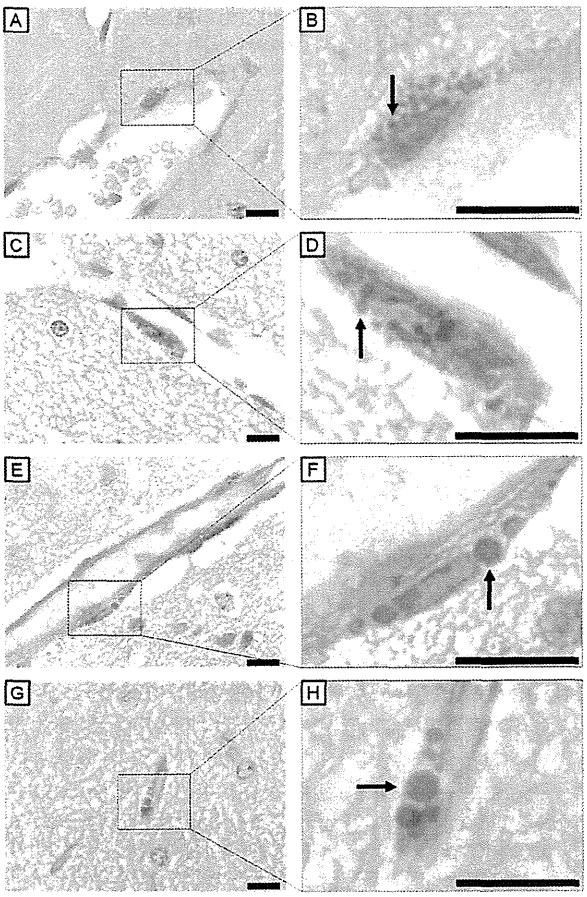

Figure 3. Light micrographs of perivascular macrophages stained with PAS-haematoxylin. All scale bars represent 10 μm. Perivascular macrophages (PVMs) surrounding cerebral blood vessels of (A, B) 6-week-old control mouse, (C, D) 12-week-old control mouse, (E, F) 6-week-old UfCB-exposed offspring mouse, and (G, H) 12-week-old UfCB-exposed offspring mouse were shown. B, D, F, H: Enlarged view of A, C, E and G: PVMs of control mice contained many PAS-positive granules, sized 0.9 μm (B, arrow) and 1.3 μm (D, arrow), in the cytoplasm. Many PAS-positive granules were enlarged in UfCB-exposed offspring (F, arrow: 2.6 μm; H, arrow: 3.0 μm).
doi:10.1371/journal.pone.0094336.g003

Number and body weight of offspring

There was no significant difference between control and UfCB-exposed offspring in number and sex ratio of pups at birth (Table 1) or their body weight at 6 and 12 weeks of age (Table 2).

Light-microscope examination of PAS staining

The intracellular granule, a feature of PVMs, was stained red with PAS [39]. For comparing the general characteristics and contents of PVMs in the offspring of maternally UfCB-exposed mice to control mice, 20 paraffin sections per mouse were observed under a light microscope. The colour photograph shows representative findings for PVMs in both control mice and UfCB-exposed offspring (Figure 3).

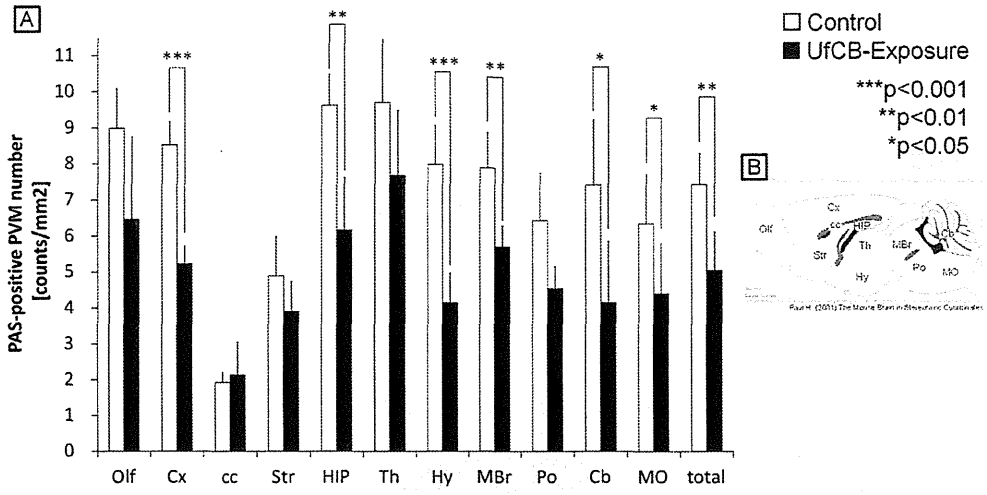

Figure 4. Quantitative observation of PAS-positive PVMs. A: The number of PAS-positive PVMs in each brain region (n = 5/group). Numbers in the following regions were significantly decreased in UfCB-exposed offspring; cerebral cortex (Cx), hippocampus (HIP), hypothalamus (Hy), midbrain (MBr), cerebellum (Cb), and medulla oblongata (MO). Asterisks indicate statistical significance (* P<0.05, **P<0.01, ***P<0.001). Data are shown as mean ±SD. B: The regions of the brain. Abbreviations: Olf, olfactory bulb; Cx, cerebral cortex; cc, corpus callosum; Str, striatum; HIP, hippocampus; Th, thalamus; Hy, hypothalamus; MBr, midbrain; Po, pons; Cb, cerebellum; MO, medulla oblongata.
doi:10.1371/journal.pone.0094336.g004

In control mice, PVMs were seen exclusively around vessels and located abluminal to endothelial cells in both 6- and 12-week-old offspring (Figure 3A, C). PVMs surrounding cerebral microvessels were slender in shape and contained many PAS-positive granules in their cytoplasm. The diameter of most of the PAS-positive granules was about 1 μm (Figure 3B, D). PAS-positive intracellular inclusions were stained weakly, and the contours of PAS-positive granules were occasionally obscure (Figure 3A, C).

In UfCB-exposed mice, the PVMs were similar in size and shape to those of the control mice, but the diameter of PAS-positive granules was larger (2–3 μm) (Figure 3F, H). Furthermore, the number of PAS-positive granules per PVM was decreased in UfCB-exposed offspring at both 6 weeks and 12 weeks of age (Figure 3F, H).

Quantitative observation of PAS-positive PVMs

For comparing the number of PVMs in UfCB-exposed offspring to control, a total of 15 paraffin sections per group were stained with PAS-haematoxylin and PAS-positive PVMs were counted under a light microscope.

In the control mice, PAS-positive PVMs around vessels numbered 7.42/mm^2 for all regions; in contrast with UfCB-exposed mice where PAS-positive PVMs numbered 5.04/mm^2 (Figure 4, Table S2). The numbers of PAS-positive PVMs were decreased in all regions of the UfCB-exposed offspring except the corpus callosum (cc); the decrease was especially significant in the cerebral cortex (Cx), hippocampus (HIP), hypothalamus (Hy), midbrain (MBr), cerebellum (Cb) and medulla oblongata (MO) (Figure 4).

Ultrastructural observation by transmission electron microscope (TEM)

Since PAS-positive granules morphologically changed and the number of PAS-positive PVMs was decreased in the UfCB group, we observed the ultrastructure of PVMs by TEM. The cerebral arterioles and venules consisted of a thin endothelium and circularly-arranged smooth muscle cells. On the outside of the vessels, the PVMs were situated between astrocytes and endothelial cells.

In control mice, most granules were round, and the contents were homogeneous and high in electron density in both 6- and 12-week-old offspring (Figure 5A, C). There were some inclusion bodies with a vacuolated structure. Only mild swelling of some astrocytic processes and end-feet was observed in the control offspring at both 6- and 12-week-old of age (Figure 5B, C). In UfCB-exposed offspring, granules with honeycomb-like structures were often found in the PVMs in 12-week-old offspring (Figure 5E). Severe swelling of astrocytic end-feet was also found adjacent to the PVMs with denatured granules in 12-week-old offspring (Figure 5E). However, the remarkable change of granules in PVMs and astrocytic end-feet was not observed in the UfCB-exposed offspring 6-week-old offspring. UfCB-like substances were not found in the offspring brains by TEM.

Relationship between PAS-positive granules and astrocytic GFAP expression

Since degeneration of astrocytic end-feet was observed in the UfCB-exposed offspring (Figure 5), we expected that the phenotype of astrocytes contacting with the vasculature was changed; we therefore analysed the expression of GFAP, which is the most commonly used phenotypic marker of astrocytes subset in the CNS, by immunohistochemistry.

In both groups, GFAP-positive astrocytes were focally prominent in the white matter (Figure 6A, C). In UfCB-exposed offspring, however, GFAP-positive astrocytes were clearly detected in the perivascular region of the grey matter (Figure 6C, D). In addition, astrocytic GFAP-positive processes completely surrounded neuronal bodies in the frontal cortex of the grey matter (Figure 6C, D).

GFAP-positive astrocytes were not observed at any sites attached to blood vessels with PVMs with small (approximately 1 μm) PAS-positive granules (Figure 7A), but were found at blood vessels with PVMs that had enlarged (approximately 2–3 μm) PAS-positive granules in the UfCB-exposed offspring (Figure 7B,

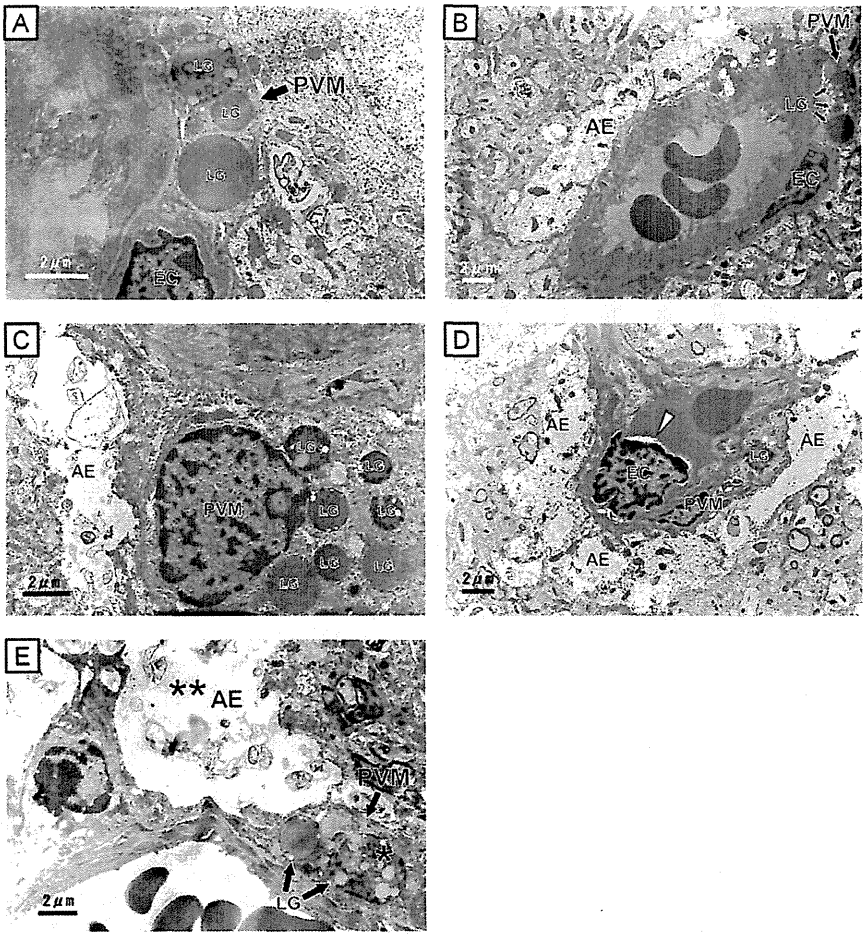

Figure 5. Transmission electron micrographs of perivascular macrophages (PVMs) and astrocytic end-foot. All scale bars represent 2 μm. A–C: Electron micrograph of perivascular regions of the cerebral cortex (grey matter) of (A, B) 6- and (C) 12-week-old mouse in the control group. (A, C) Perivascular macrophages [PVM] were found between endothelial cells and glia limitans with many round lysosomal granules [LG] of moderate intensity and some pale vacuoles. (B, C) The astrocytic end-foot [AE] was attached to a endothelial cells [EC] and a perivascular macrophage. D, E: Electron micrographs of perivascular regions of the cerebral cortex (grey matter) of (D) 6- and (E) 12-week-old UfCB-exposed offspring mouse. (D) Arrow head: Crescent-shaped spaces, an ultrastructural feature of apoptotic bodies [57], of EC were shown. (E) Honeycomb-like structured lysosomal granules (*) were shown in the perivascular macrophages [PVM]. (E) Severe swelling of astrocytic end-feet (**) was found at sites attached to perivascular macrophages with denatured granules.
doi:10.1371/journal.pone.0094336.g005

C). Moreover, GFAP-positive astrocytic end-feet were detected at sites attached to PVMs with enlarged PAS-positive granules (Figure 7E, G, H), and not surrounding PVMs with small PAS-positive granules (Figure 7F, I) around one blood vessel in the UfCB-exposed offspring (Figure 7D–I). These results suggested that the increase in the expression level of GFAP in astrocytic end-feet around blood vessels in the grey matter was correlated with enlargement of PAS-positive granules of PVM.

Discussion

In the present study, we examined the effect of maternal exposure to UfCB on PVMs and surrounding tissue in murine CNS using PAS staining, transmission electron microscopy and GFAP immunohistochemistry. First, we counted PAS-positive PVMs quantitatively in each brain region with a simple method for staining large quantities of tissue sections uniformly and entirely. PAS staining can selectively detect PVMs and meningeal macrophages in the CNS. Only the PAS-positive cells located with blood vessels in the brain parenchyma were counted in order to quantitatively analyse the PVMs in the CNS. Although we can detect murine and human PVMs with scavenger receptors (CD204, CD163) [2,15], these molecules are not so selective because it is also expressed on the microglia in the CNS, especially under inflammatory conditions [15,40]. Previous studies have suggested that PVMs were predominantly present in the grey matter and that the corpus callosum, one of the typical regions in the white matter, had a smaller number of PVMs [1]. The number of PVMs was positively correlated with capillary density in each region. Our quantitative data showed that the frequency of PAS-positive PVM appearance was 4-fold higher in the cerebral cortex than in the corpus callosum; likewise, capillary density was also reported to be about 4-fold higher in the cerebral cortex than in the corpus callosum [41]. PVMs are positive for PAS in physiological and mild-pathologic conditions such as Tay-Sachs

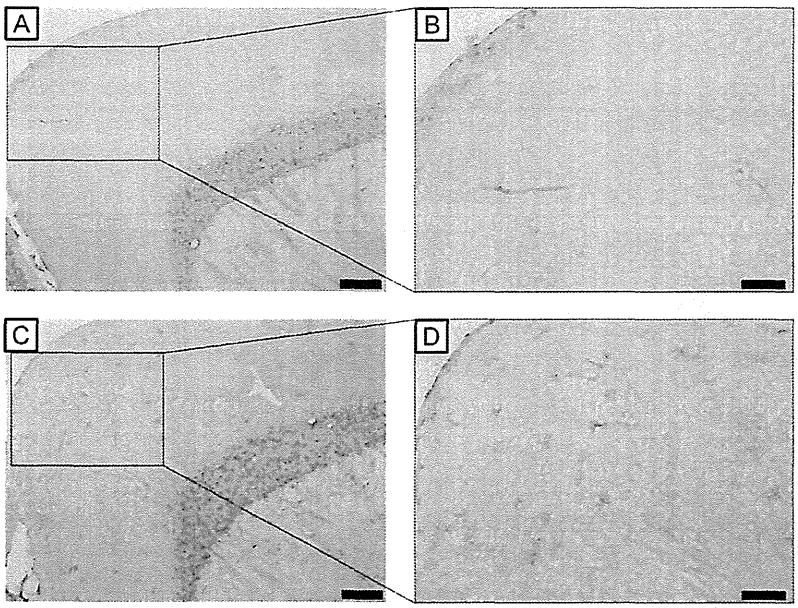

Figure 6. Light micrographs of GFAP-positive astrocytes of the wide-field. Scale bars represent (A, C) 200 m or (B, D) 100 m. A, C: The frontal cortex of 6-week-old male mice of (A) the control group (B) UfCB-exposed offspring. B, D: Enlarged views of A and C. (B) Few GFAP-positive astrocytes were observed in the grey matter in the control group, while (D) many GFAP-positive astrocytes were detected in the grey matter in UfCB-exposed offspring. GFAP-positive astrocytes were not observed at any sites attached to blood vessels with PVMs with small (approximately 1 m) PAS-positive granules (Figure 7A), but were found at blood vessels with PVMs that had enlarged (approximately 2-3 m) PAS-positive granules in the UfCB-exposed offspring (Figure 7B, C). Moreover, GFAP-positive astrocytic end-feet were detected at sites attached to PVMs with enlarged PAS-positive granules (Figure 7E, G, H), and not surrounding PVMs with small PAS-positive granules (Figure 7F, I) around one blood vessel in the UfCB-exposed offspring (Figure 7D-I). These results suggested that the increase in the expression level of GFAP in astrocytic end-feet around blood vessels in the grey matter was correlated with enlargement of PAS-positive granules of PVM .
doi:10.1371/journal.pone.0094336.g006

disease [42], but may be negative for PAS when they are severely degenerated in conditions such as Sandhoff's disease [42]. On the other hand, the number of PVMs are greatly increased and accumulated around blood vessels in experimental allergic encephalomyelitis [8].

Our data showed that PVM granules were enlarged and that the number of PAS-positive PVMs indicated a decrease in "normal" PVMs in a wide area of the CNS after maternal UfCB exposure. Generally, PVM granules are enlarged in mild pathological and aging conditions [42,43,44], presumably by the uptake and accumulation of substances from plasma [43]. More severely denatured PVMs cannot retain spherical (lipid and waste products) granules, and PAS-positive granules have been shown to become negative for PAS-staining [42,45]. These reports suggest that a decrease in PAS-positive PVMs is generally well-correlated with dysfunction of the cells. Furthermore, our electron microscopy results, where some honeycomb-like structures were observed in the granule, support the denaturation of PVM granules after growth (12-week-old offspring) in the UfCB group.

An increase in GFAP expression in the cells surrounding blood vessels in the cerebral cortex suggested that the blood vessels may be damaged in UfCB-exposed offspring. GFAP is an intermediate filament protein, which is the most common phenotypic marker labelling of astrocytes under conditions of denaturation or inflammation [46,47]. Astrocytes highly express GFAP in their end-feet and extend it to injured regions, where cerebral blood vessels or neuronal cells are injured in pathological conditions such as infection and transient ischemia [46,48,49]. In addition, the swelling of astrocytic end-feet in UfCB-exposed offspring, as observed by electron microscopy, was similar to a feature of ischemia-related blood vessel damage [46,47]. These data also suggest that maternal UfCB exposure induces persisting alteration of the phenotype of PVMs and attached astrocytes in the brains of mouse offspring.

Interestingly, the increase in astrocytic GFAP expression level was closely related to the enlargement of granules in the attached PVMs. A decrease in the number of normal PVMs suggests PVM dysfunction in the UfCB group, the cause of which may be the invasion of foreign matter or pathogens to the brain parenchyma [3,43], accumulation of waste products [3], a decrease in immunocompetence in the surrounding blood vessels [3,13], and/or damage to blood vessels and weakening of the BBB function [15]. To protect against and restrict the spread of infectious agents and inflammatory cells in the CNS parenchyma, an astrocyte extends its end-foot to the vessel when there is an increase in the expression level of astrocytic GFAP [46,49]. PVMs with enlarged granules may be associated with the attraction of astrocytic end-feet toward themselves in UfCB-exposed offspring. GFAP-positive astrocytic end-feet were observed around PVMs with enlarged granules.

The present study also contributed to elucidating the mechanism underlying the effect of maternal exposure to ultrafine particles in the atmospheric environment. It is well-known that the core of combustion-derived particles is composed of UfCB [50], which represents relevant surrogate model particles for airborne fine ($PM_{2.5}$) and ultrafine particles [51]. Further investigation is needed to clarify which direct or indirect effect of UfCB is the main contributor to the effect on PVMs and surrounding astrocytes in mouse offspring. Ultrafine particles with a diameter of $<$200 nm may transfer from the pregnant body to offspring by passing through the placenta [29,52] and may directly affect the development of offspring. Alteration in the pregnant body, such as

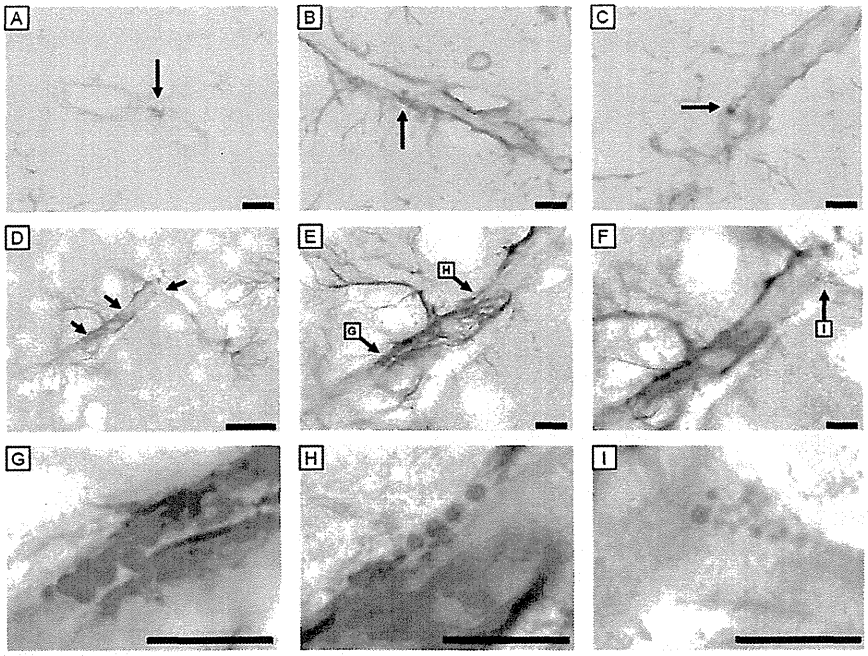

Figure 7. Light micrographs of GFAP-positive astrocytes and PAS-positive PVMs of 6-week-old male mice. All scale bars represent 10 μm. (A–C) 6-μm paraffin sections and (D–I) 10-μm frozen sections. A: PVM surrounding the cerebral blood vessels of a 6-week-old control mouse. GFAP-positive astrocytes were very few in number at sites attached to blood vessels with PVMs with small (approximately 1 μm) PAS-positive granules (arrow). B, C: PVM surrounding cerebral blood vessels of a mouse in the UfCB group. The PVM possessed enlarged granules (arrows). Many GFAP-positive astrocytes were observed at sites attached to PVMs with enlarged granules. D: GFAP-positive astrocytes and PAS-positive PVM (arrows) surrounding cerebral blood vessels of mouse in the UfCB group. E–I: Enlarged views of (D). Around one cerebral vessel, GFAP-positive astrocytic end-feet were detected (E, G, H) at a site attached to PVM with enlarged PAS-positive granules (G, 2.2 μm; H, 1.6 μm), but (F, I) not surrounding PVMs with small PAS-positive granules (smaller than 1.1 μm).
doi:10.1371/journal.pone.0094336.g007

an increase in circulating cytokines or other secondary messengers that are activated in response to inflammation and/or oxidative stress, may also influence the development [53,54,55]. Our results demonstrate the need to find a means of preventing and controlling the developmental effect of maternal exposure to ultrafine particles on the CNS, especially in the maintenance of brain perivascular regions. The previous study reported that the changes of gene expression in olfactory bulb, where is one of the brain region, by exposure to diesel exhaust were prevented by enrichment rearing environment [56]. The living environment during perinatal period is of interest for preventing the development effects of ultrafineparticles.

In summary, the present study showed that exposure of pregnant mothers to UfCB degenerated PVM granules and decreased the number of normal PVMs of offspring. An increase in the expression level of GFAP was also shown in the astrocytes surrounding PVMs with enlarged granules in UfCB-exposed offspring. The phenotypic changes in PVMs and astrocytes indicate that maternal UfCB exposure may alter brain blood vessels and be associated with the risk of brain dysfunction and disorders in future offspring. It would be necessary to clarify the mechanisms underlying the effect of UfCB on the astrocytes and CNS function of offspring.

Supporting Information

Table S1 Total number of PAS-positive PVMs in each sample.
(DOC)

Table S2 Number of PAS-positive PVMs in each brain region. Data are presented as mean ± SD. Abbreviations: Olf, olfactory bulb; Cx, cerebral cortex; cc, corpus callosum; Str, striatum; HIP, hippocampus; Th, thalamus; Hy, hypothalamus; MBr, midbrain; Po, pons; Cb, cerebellum; MO, medulla oblongata.
(DOC)

Author Contributions

Conceived and designed the experiments: KT MU AO. Performed the experiments: AO MS TI. Analyzed the data: AO MU MS. Wrote the paper: AO MU.

References

1. Galea I, Palin K, Newman TA, Van Rooijen N, Perry VH, et al. (2005) Mannose receptor expression specifically reveals perivascular macrophages in normal, injured, and diseased mouse brain. Glia 49:375–384.
2. Kim WK, Alvarez X, Fisher J, Bronfin B, Westmoreland S, et al. (2006) CD163 identifies perivascular macrophages in normal and viral encephalitic brains and potential precursors to perivascular macrophages in blood. Am J Pathol 168:822–834.
3. Williams K, Alvarez X, Lackner AA (2001) Central nervous system perivascular cells are immunoregulatory cells that connect the CNS with the peripheral immune system. Glia 36:156–164.

4. Peters A, Palay SL, Webster HD (1976) The fine structure of thenervous system: the neurons and supporting cells. Philadelphia: WB Saunders.
5. Graeber MB, Streit WJ, Buringer D, Sparks DL, Kreutzberg GW (1992) Ultrastructural location of major histocompatibility complex(MHC) class II positive perivascular cells in histologically normal human brain. J Neuropathol Exp Neurol 51:303–311.
6. Streit WJ, Graeber MB (1993) Heterogeneity of microglial and perivascular cell populations: insights gained from the facial nucleus paradigm. Glia 7:68–74.
7. Lassmann H, Zimprich F, Vass K, Hickey WF (1991) Microglial cells are a component of the perivascular glia limitans. J Neurosci Res 28:236–243.
8. Lassmann H, Schmied M, Vass K, Hickey WF (1993) Bone marrow derived elements and resident microglia in brain inflammation. Glia 7:19–24.
9. Cserr HF, Ostrach LH (1974) Bulk flow of interstitial fluid after intracranial injection of blue dextran 2000. Exp Neurol 45(1):50–60.
10. Weller RO, Kida S, Zhang ET (1992) Pathways of fluid drainage from the brain—morphological aspects and immunological significance in rat and man. Brain Pathol 2(4):277–84.
11. Zhang ET, Richards HK, Kida S, Weller RO (1992) Directional and compartmentalised drainage of interstitial fluid and cerebrospinal fluid from the rat brain. Acta Neuropathol 83(3):233–9.
12. Iliff JJ, Wang M, Liao Y, Plogg BA, Peng W, et al. (2012) A paravascular pathway facilitates CSF flow through the brain parenchyma and the clearance of interstitial solutes, including amyloid β. Sci Transl Med 15;4(147):147
13. Serrats J, Schiltz JC, García-Bueno B, van Rooijen N, Reyes TM, et al. (2010) Dual roles for perivascular macrophages in immune-to-brain signaling. Neuron 65:94–106.
14. Kida S, Steart PV, Zhang ET, Weller RO (1993) Perivascular cells act as scavengers in the cerebral perivascular spaces and remain distinct from pericytes, microglia and macrophages. Acta Neuropathol (Berl) 85:646–652.
15. Fabriek BO, Van Haastert ES, Galea I, Polfliet MM, Döpp ED, et al. (2005) CD163-positive perivascular macrophages in the human CNS express molecules for antigen recognition and presentation. Glia 51:297–305.
16. Donaldson K, Tran L, Jimenez LA, Duffin R, Newby DE, et al. (2005) Combustion-derived nanoparticles: a review of their toxicology following inhalation exposure. Part Fibre Toxicol 21;2:10.
17. Oberdörster G, Oberdörster E, Oberdörster J (2005) Nanotoxicology: an emerging discipline evolving from studies of ultrafine particles. Environ Health Perspect 113(7):823–39.
18. Nel A, Xia T, Mädler L, Li N (2006) Toxic potential of materials at the nanolevel. Science 3;311(5761):622–7.
19. Tin-Tin-Win-Shwe, Yamamoto S, Ahmed S, Kakeyama M, Kobayashi T, et al. (2006) Brain cytokine and chemokine mRNA expression in mice induced by intranasal instillation with ultrafine carbon black. Toxicol Lett 25;163(2):153–60.
20. Vesterdal LK, Folkmann JK, Jacobsen NR, Sheykhzade M, Wallin H, et al. (2010) Pulmonary exposure to carbon black nanoparticles and vascular effects. Part Fibre Toxicol 5;7:33.
21. Peters K, Unger RE, Kirkpatrick CJ, Gatti AM, Monari E (2004) Effects of nano-scaled particles on endothelial cell function in vitro: studies on viability, proliferation and inflammation. J Mater Sci Mater Med 15(4):321–5.
22. Duffin R, Tran L, Brown D, Stone V, Donaldson K (2007) Proinflammogenic effects of low-toxicity and metal nanoparticles in vivo and in vitro: highlighting the role of particle surface area and surface reactivity. Inhal Toxicol 19; 849–856.
23. Stone V, Johnston H, Clift MJ (2007) Air pollution, ultrafine and nanoparticle toxicology: cellular and molecular interactions. IEEE Trans Nanobiosci 6; 331–340.
24. Brown DM, Stone V, Findlay P, MacNee W, Donaldson K (2000) Increased inflammation and intracellular calcium caused by ultrafine carbon black is independent of transition metals or other soluble components. Occup Environ 57, 685–691.
25. Jacobsen NR, Moller P, Jensen KA, Vogel U, Ladefoged O, et al. (2009) Lung inflammation and genotoxicity following pulmonary exposure to nanoparticles in ApoE-/- mice. Part Toxicol. 12; 6, 2.
26. Wilson MR, Lightbody JH, Donaldson K, Sales J, Stone V (2002) Interactions between ultrafine particles and transition metals in vivo and in vitro. Toxicol Appl Pharmacol. 184, 172–179.
27. Oberdörster G, Sharp Z, Atudorei V, Elder A, Gelein R, et al. (2002) Extrapulmonary translocation of ultrafine carbon particles following whole-body inhalation exposure of rats. J Toxicol Environ Health A 65: 1531–1543
28. Kreyling WG, Semmler M, Erbe F, Mayer P, Takenaka S, et al. (2002) Translocation of ultrafine insoluble iridium particles from lung epithelium to extrapulmonary organs is size dependent but very low. J Toxicol Environ Health A 65: 1513–1530
29. Takeda K, Suzuki K, Ishihara A, Kubo-Irie M, Fujimoto R, T, et al. (2009) Nanoparticles transferred from pregnant mice to their offspring can damage the genital and cranial nerve systems. Jounal if Health Science 55(1) 95–102
30. Sugamata M, Ihara T, Takano H, Oshio S, Takeda K (2006) Maternal Diesel Exhaust Exposure Damages Newborn Murine Brains. Journal of Health Science 52:82–84
31. Jackson P, Vogel U, Wallin H, Hougaard KS (2011) Maternal Exposure to Particulate Air Pollution and Engineered Nanoparticles: Reproductive and Developmental Effects. In: Anca, M M, editor. Air Pollution - New Developments. Rijeka University Campus Step Ri. pp. 59–84.
32. Saber AT, Jensen KA, Jacobsen NR, Birkedal R, Mikkelsen L, et al. (2011) Inflammatory and genotoxic effects of nanoparticles designed for inclusion in paints and lacquers. Nanotoxicology 6(3):453–71.
33. Jacobsen NR, Saber AT, White P, Møller P, Pojana G, et al. (2007) Increased mutant frequency by carbon black, but not quartz, in the lacZ and cII transgenes of muta mouse lung epithelial cells. Environ Mol Mutagen 48(6):451–61.
34. Jacobsen NR, White PA, Gingerich J, Møller P, Saber AT, et al. (2011) Mutation spectrum in FE1-MUTA(TM) Mouse lung epithelial cells exposed to nanoparticulate carbon black. Environ Mol Mutagen 52(4):331–7.
35. Wilson JG (1972) Environmental effects on development-teratology. In: N F Affli, editor. Pathophysiology of gestation, vol. II. New York: Academic. pp. 270–320.
36. Pietroiusti A1, Massimiani M, Fenoglio I, Colonna M, Valentini F, et al. (2011) Low doses of pristine and oxidized single-wall carbon nanotubes affect mammalian embryonic development. ACS Nano. 28;5(6):4624–33.
37. Umezawa M, Kudo S, Yanagita S, Shinkai Y, Niki R, et al. (2011) Maternal exposure to carbon black nanoparticle increases collagen type VIII expression in the kidney of offspring. J Toxicol Sci. 36(4):461–8.
38. Kilkenny C, Browne W, Cuthill IC, Emerson M, Altman DG (2010) Animal research: reporting in vivo experiments: the ARRIVE guidelines. Br J Pharmacol 160: 1577–1579.
39. Mato M, Ookawara S (1979) A simple method for observation of capillary nets in rat brain cortex. Experientia 15;35(4):501–3.
40. Guillemin GJ, Brew BJ (2004) Microglia, macrophages, perivascular macrophages, and pericytes: a review of function and identification. J Leukoc Biol 75(3):388–97.
41. Cavaglia M, Dombrowski SM, Drazba J, Vasanji A, Bokesch PM, et al. (2001) Regional variation in brain capillary density and vascular response to ischemia. Brain Res 10;910(1–2):81–93.
42. Mato M, Takeuchi K, Ookawara S, Yamanaka S, Mashiko T, et al. (2002) Inclusions in novel perivascular macrophages (Mato's fluorescent granular perithelial cells) and neurons in the cerebral cortex of Hex A- and Hex B-deficient mice. Acta Neuropathol 103:119–130.
43. Mato M, Ookawara S, Sakamoto A, Aikawa E, Ogawa T, et al. (1996) Involvement of specific macrophage-lineage cells surrounding arterioles in barrier and scavenger function in brain cortex. Proc Natl Acad Sci U S A 93:3269–3274.
44. Nakazawa T, Yamamura H, Shimizu S, Nishikawa M, Ezaki T, et al. (2006) Acceleration of Age-related Changes in the Granules of Perivascular Macrophages from the Brain of Senescence Accelerated Mice (SAM). J Tokyo Wom Med Univ 76: 82–91.
45. Mato T, Kamei M, Ito R, Sawano M, Inokuchi K, et al. (2009) Beneficial Effects of Cocoa in Perivascular Mato Cells of Cerebral Arterioles in SHR-SP (Izm) Rats. J Clin Biochem Nutr 44:142–150.
46. Sofroniew MV, Vinters HV (2010) Astrocytes: biology and pathology. Acta Neuropathol 119:7–35.
47. Molofsky AV, Krencik R, Ullian EM, Tsai HH, Deneen B, et al. (2012) Astrocytes and disease: a neurodevelopmental perspective. Genes Dev 26:891–907.
48. Klatzo I (1976) Presidental address. Neuropathological aspects of brain edema. J Neuropathol Exp Neurol 1967. 26:1–14.
49. Tsai HH, Li H, Fuentealba LC, Molofsky AV, Taveira-Marques R, et al. (2012) Regional astrocyte allocation regulates CNS synaptogenesis and repair. Science 337(6092):358–62.
50. BéruBé K, Balharry D, Sexton K, Koshy L, Jones T (2007) Combustion-derived nanoparticles: mechanisms of pulmonary toxicity. Clin Exp Pharmacol Physiol 34(10):1044–50.
51. Stoeger T, Takenaka S, Frankenberger B, Ritter B, Karg E, et al. (2009) Deducing in vivo toxicity of combustion-derived nanoparticles from a cell-free oxidative potency assay and metabolic activation of organic compounds. Environ Health Perspect 117(1):54–60.
52. Wick P, Malek A, Manser P, Meili D, Maeder-Althaus X, et al. (2010) Barrier capacity of human placenta for nanosized materials. Environ Health Perspect 118(3):432–6.
53. Hougaard KS, Fadeel B, Gulumian M, Kagan VE, Savolainen KM (2011) Developmental toxicity of engineered nanoparticles. In: Ramesh CG, editor. Reproductive and Developmental Toxicology. Academic Press, San Diego. pp. 269–290.
54. Jackson P, Hougaard KS, Boisen AM, Jacobsen NR, Jensen KA, et al. (2012) Pulmonary exposure to carbon black by inhalation or instillation in pregnant mice: effects on liver DNA strand breaks in dams and offspring. Nanotoxicology 6(5):486–500.
55. Kannan S, Misra DP, Dvonch JT, Krishnakumar A (2007) Exposures to airborne particulate matter and adverse perinatal outcomes: a biologically plausible mechanistic framework for exploring potential. Cien. Saude Colet. 12, 1591–1602.
56. Yokota S, Hori H, Umezawa M, Kubota N, Niki R, et al. (2013) Gene expression changes in the olfactory bulb of mice induced by exposure to diesel exhaust are dependent on animal rearing environment. PLoS One 5;8 (8)
57. Ihara T, Yamamoto T, Sugamata M, Okumura H, Ueno Y (1998) The process of ultrastructural changes from nuclei to apoptotic body. Virchows Arch 433(5):443–7.

J Nanopart Res (2014) 16:2284
DOI 10.1007/s11051-014-2284-7

RESEARCH PAPER

Dose–dependent biodistribution of prenatal exposure to rutile-type titanium dioxide nanoparticles on mouse testis

Miyoko Kubo-Irie · Hiroki Uchida · Shotaro Mastuzawa · Yasuko Yoshida · Yusuke Shinkai · Kenichiro Suzuki · Satoshi Yokota · Shigeru Oshio · Ken Takeda

Received: 19 September 2013 / Accepted: 17 January 2014

Abstract Titanium dioxide nanoparticles (nano-TiO_2), believed to be inert and safe, are used in many products especially rutile-type in cosmetics. Detection, localization, and count of nanoparticles in tissue sections are of considerable current interest. Here, we evaluate the dose–dependent biodistribution of rutile-type nano-TiO_2 exposure during pregnancy on offspring testes. Pregnant mice were subcutaneously injected five times with 0.1 ml of sequentially diluted of nano-TiO_2 powder, 35 nm with primary diameter, suspensions (1, 10, 100, or 1,000 μg/ml), and received total doses of 0.5, 5, 50, and 500 μg, respectively. Prior to injection, the size distribution of nano-TiO_2 was analyzed by dynamic light scattering measurement. The average diameter was increased in a dose–dependent manner. The most diluted concentration, 1 μg/ml suspension, contained small agglomerates averaging 193.3 ± 5.4 nm in diameter. The offspring testes were examined at 12 weeks postpartum. Individual particle analysis in testicular sections under scanning and transmission electron microscopy enabled us to understand the biodistribution. The correlation between nano-TiO_2 doses injected to pregnant mice, and the number of agglomerates in the offspring testes was demonstrated to be dose–dependent by semiquantitative evaluation. However, the agglomerate size was below 200 nm in the testicular sections of all recipient groups, independent from the injected dose during pregnancy.

Keywords Rutile-type nano-TiO_2 · Agglomerates · Dose–dependence · Prenatal exposure · Offspring testis · In-vivo testing · Nanomedicine

M. Kubo-Irie (✉) · H. Uchida · S. Mastuzawa · Y. Yoshida · Y. Shinkai · S. Yokota · K. Takeda
Department of Hygiene Chemistry, Faculty of Pharmaceutical Science, Tokyo University of Science, 2641 Yamazaki, Noda-shi, Chiba 278-8510, Japan
e-mail: miyoko_kubo_irie@hotmail.com

K. Takeda
e-mail: takedak@rs.noda.tus.ac.jp

M. Kubo-Irie
Biological Laboratory, University of the Air, 2-11 Wakaba, Mihama-Ku, Chiba 261-8586, Japan

K. Suzuki · K. Takeda
Center for Environmental Health Science for the Next Generation, Research Institute for Science and Technology, Tokyo University of Science, 2641 Yamazaki, Noda-shi, Chiba 278-8510, Japan

S. Oshio
Department of Hygiene Chemistry, Ohu University School of Pharmaceutical Sciences, 31-1 Misumido, Tomita-machi, Kohriyama-shi, Fukushima 963-8611, Japan

Introduction

Titanium dioxide nanoparticles (nano-TiO_2) are manufactured worldwide in large quantities for use in many products such as paints, plastics, papers, inks,

Published online: 01 February 2014